Microfluidic removal of teratoma-forming cells from hiPSC-derived Neural Progenitor Cells

Kyle Wellmerling[1,*], Christian Lehmann[1], Ankur Singh[1,2], and Brian Kirby[1,3]

[1]Sibley School of Mechanical and Aerospace Engineering, Cornell University, Ithaca NY, 14853, United States
[2]Meinig School of Biomedical Engineering, Cornell University, Ithaca NY, 14853, United States
[3]Division of Hematology and Medical Oncology Weill–Cornell Medicine, New York NY, 10075, United States
[*]corresponding author: kirby@cornell.edu

ABSTRACT

Teratoma formation remains a safety concern in therapeutic cell populations derived from human-induced pluripotent stem cells. Here we employ a microfluidic geometrically enhanced differential immunocapture device to remove cells with teratoma-forming potential from a differentiating population of human-induced pluripotent stem cell-derived Neural progenitor cells and overcome the limitations of current teratoma-preventing methods. We demonstrate that the geometrically enhanced differential immunocapture device successfully reduces the teratoma-forming potential of the human-induced pluripotent stem cell-derived neural progenitor cell population, and can be used as a tool to enhance human-induced pluripotent stem cell-derived cell population safety prior to therapeutic transplantation.

Introduction

Pluripotent stem cells (PSCs) represent a highly promising strategy to derive cells for therapeutic transplantation [1, 2]. Of these, human-induced PSCs (hiPSCs) are particularly exciting, because they (1) generate patient-specific tissue, which is thought to be less immunogenic than tissue derived from non-allogenic human embryonic stem cells (hESCs) [3] (2) circumvent harvesting hESCs from unborn fetuses and concomitant ethical questions, and (3) self-renew indefinitely, enabling derivation of the large number of cells required for therapeutic transplantation [4]. Of tissue derived from hiPSCs, neural stem and progenitor cells (NSPCs) are a promising therapy for treating chronic neurodegenerative diseases, for example Alzheimer′s disease (AD), which affects 5.7 million Americans and costs $277 billion per year to treat as of 2018, and Parkinson's disease (PD), which affects 630,000 Americans and costs $14.4 billion per year to treat as of 2010[5, 6]. Further, since PD and AD are age related diseases, and the potential for impact is expected to rise as population demographics age. NPCs are a promising strategy to treat AD and PD, as AD and PD both constitute a widespread loss of neurons [7, 8]. Current treatments primarily focus on administering neurotransmitters to stimulate signaling [9, 10], and are unfortunately temporary, providing symptomatic relief rather than halting disease progression. However, cell transplant therapies which enhance neurogenesis or replace lost neurons may delay the progression of AD and PD. NPC grafts onto rodent models of AD demonstrate increased hippocampal synaptic density and increased cognitive function [7, 11]. Additionally, cellular therapies used fetal ventral midbrain tissue as a source of dopaminergic (DA) neurons[7], and reported varying degrees of success [12]. However, cellular transplants utilizing fetal ventral midbrain tissue are limited due to ethical concerns of harvesting cells from unborn fetuses and the inability to obtain adequate numbers of cells for transplant[7]. hiPSC-derived NPCs (hiPSC-NPCs) are poised to overcome these obstacles and have demonstrated cell integration into host tissue in a rodent PD model[7, 13]. In addition to chronic neurodegenerative diseases, acute neurodegeneration may result from traumatic brain injury (TBI), stroke, or spinal cord injury. In the US approximately 5 million people are living with a TBI-related long-term disability, costing $76.5 billion annually through missed work, 795,000 people have a stroke each year, costing $70 billion annually, and 253,000 people live with a spinal cord injury disability, costing $7.0 billion annually[14–16]. Human NPC transplantation has shown promising results to treat TBI and has demonstrated neuroprotection and improved cognitive outcomes following TBI[17]. Human NSC transplantation has been shown to promote functional recovery in rats with intracerebral hemorrhage stroke model[18, 19], and hESC-derived neural precursor cell transplants have shown functional recovery in cortical stroke rats. Further, hiPSC-NPCs have demonstrated motor functional recovery in mice[20]. Taken together, these results demonstrate that NPCs are a promising method to treat acute neurodegeneration in humans. Despite the promise of hiPSCs derived cells to treat disease, tumorigenicity remains a concern[21**?** –24]. At present, numerous techniques have been applied to remove teratoma-forming potential from hiPSC-derived products, such as pretreatment with antimitotic agents and delayed transplant[25], sorting with FACS[26], MACS[27], introduction of inducible suicide genes[28], and complete differentiation into mature DA neurons[29]. Unfortunately, each

of these methods has its shortfalls. Pretreatment with antimitotic agents and delayed transplant or complete differentiation into mature dopaminergic neurons will increase turn around time to derive therapeutic cells, and could make it difficult to transplant cells during the 1-2 week window subacute phase of acute neurodegenerative disorders[20]. Inducible suicide genes only respond in 95% of cells[28], which by itself is unlikely to eliminate teratoma concerns, as 2 ESCs in two million non-neoplastic cells form tumors in 60% of transplants[25]. Additionally, FACS and MACS have thus far proven insufficient to eliminate teratoma-forming potential[26, 27], FACS leads to low recovery of sorted cells[27], and both require pre-labeling cells with antibodies which could interfere with proliferation and differentiation[27, 30, 31]. However, microfluidic devices represent a potential avenue to remove rare, teratoma-forming cells. Microfluidic devices have shown effective capture of rare circulating tumor cells (CTCs) from whole blood[32], indicating their potential to remove rare cells from a cell population. Further, microfluidic devices have demonstrated enrichment and high survivability of mouse stem cells[33]. To this end we have engineered a geometrically enhanced differential immunocapture (GEDI) device to capture and remove rare, teratoma-forming cells from a hiPSC-derived NPC population (figure 2a). This GEDI device exploits size to maximize the number of collisions a cell experiences with an antibody functionalized post (figure 2b and 2c). Device geometry is designed such that cells above a set size follow a pathline through the device that causes repeated collision with the antibody functionalized posts. To remove cells from a hiPSC-derived NPC population, cells are first differentiated on a culture plate, resuspended as a single-cell suspension, then teratoma-forming cells are captured by antibodies on the chip surface, and a purified population is obtained in the effluent (figure 1d). Further, given the recent discovery of the pluripotency surface marker SSEA-5, which has higher dynamic range in expression than older surface markers such as SSEA-3 or TRA-1-60[26], we believe microfluidic immunocapture represents a promising tool to address the tumorigenic potential of hiPSC-derived cell cultures.

1 Results

1.1 Differentiation of hiPSCs into NPCs

To design a device that removes teratoma-forming cells from a hiPSC-derived NPCs we first sought to characterize the differentiation dynamics of hiPSCs. Chiefly, we sought to characterize how SSEA-5 expression changes during differentiation, as SSEA-5 was our principal marker for teratoma-forming potential. We used flow cytometry to measure single-cell SSEA-5 expression at different time points of differentiation and measured the percent of the population SSEA-5$^+$ at each time point of differentiation (figure 1a). During differentiation we note that SSEA-5 expression decreases dramatically throughout the 12-day differentiation period (Figure 1b,c). Further, we note that SSEA-5 population drops at discrete intervals rather than continuously during the differentiation process. SSEA-5 expression is roughly constant during the first 3 days of differentiation then drops dramatically during day 4. SSEA-5 expression remains relatively constant again through day 6 and drops dramatically again between day 6 and day 9. SSEA-5 expression then levels off after day 9, indicating most cells have completed differentiation.

However, despite the drop in average SSEA-5 expression, we sought to investigate a potential residual population of pluripotent or partially-differentiated cells with teratoma-forming potential. For each time point of differentiation we found the percent of the population with SSEA-5 expression above the bottom 5% of undifferentiated hiPSCs. We designated this fraction SSEA-5$^+$ (figure 1d). Strikingly, we note that on day 12 of differentiation, 1% of the cells are SSEA-5$^+$ after a full time-course of differentiation. It is unlikely this small fraction of cells represents noise in the flow cytometry data because BxPC3s stained for SSEA-5 only showed 0.04% of the population being SSEA-5$^+$. Further similar numbers are obtained when experiments were performed using a single antibody conjugated to a fluorophore to measure SSEA-5 expression (supplementary figure 1b). This suggests there is a residual population of hiPSC-NPCs with a pluripotency signature and thus teratoma-forming potential. This data is further backed up by repeated experiments in which a single antibody conjugated to a fluorophore was used, instead of a primary and secondary antibody (supplementary figure 1b). To further investigate these cell populations we plotted the skew of SSEA-5 expression at each time point of differentiation. Interestingly, the differentiating cells are initially skewed towards low SSEA-5 expression (negative skew), indicating a few cells lose pluripotency faster than the rest of the population. Later on however, at day 9 and day 12 the skew becomes positive (skewed towards high SSEA-5). This indicates at the later stages of differentiation there are cells slow to differentiate that retain pluripotency expression. Finally, to corroborate flow cytometry data with immunofluorescence (IF) images (figure 1f), we stained undifferentiated hiPSCs and day 9 hiPSC-NPCs with Oct4, a master regulator of pluripotency, SSEA-5, and Nestin (a marker of neural differentiation, but reported in iPSCs[34]). Strikingly, IF images corroborate flow data, clearly indicating that pockets of cells with high SSEA-5 expression remain on day 9, though with weak Oct4 expression, suggesting the cells are not fully pluripotent, but may retain some pluripotential.

1.2 Microfluidic immunocapture of teratoma-forming cells

Having confirmed the presence of residual cells with expression of pluripotency markers and thus teratoma-forming potential, we sought to employ a microfluidic GEDI device to remove the teratoma-forming cells from hiPSC-NPCs. To demonstrate SSEA-5 as a pluripotency surface marker (PSM) capable of capturing hiPSCs on a GEDI device, we first qualitatively compared

capture on glass coverslips functionalized with anti-SSEA-5, anti-TRA-1-60, and normal mouse IgG antibodies (isotype control) (to test for steric hindrance (Figure 3a). Qualitatively we noticed similar numbers of cells on the anti-SSEA-5 and anti-TRA-1-60 coverslips compared with the isotype control cover slips. Knowing that anti-SSEA-5 and anti-TRA-1-60 coverslips capture hiPSC, we tested functionalized GEDI chips with each of the three above antibody functionalizations respectively, and a combination of anti-SSEA-5 plus anti-TRA-1-60 functionalized on the same GEDI chip. Undifferentiated hiPSCs were pumped through the GEDI chips at approximately 300 cells/ml (see Figure 1d).A *pass-through rate* was then calculated based on the number of cells counted in the effluent of each chip: $\frac{number\ of\ cells\ in\ effluent}{number\ of\ cells\ loaded}$

Observed pass-through rates are shown in figure 3b. Whereas anti-SSEA-5 and anti-TRA-1-60 GEDI chips had similar pass-through rates, the isotype-control GEDI chips had a much higher pass-through rate, indicating both anti-SSEA-5 and anti-TRA-1-60 GEDI chips capture hiPSCs preferentially compared with a control. Given the anti-SSEA-5 GEDI chips had the lowest overall pass-through rate we chose to focus on this antibody for future experiments.

1.3 Capture based on SSEA-5 expression

After confirming SSEA-5 expression exists in differentiated hiPSC-NPCs we sought to confirm our device's ability to remove SSEA-5+ cells from a largely SSEA-5- population, in a manner proportional to SSEA-5 expression level of the target population. To demonstrate this capability, we spiked hiPSC-NPCs (300 cells/ml) differentiated for a set number of days into a population of 300,000 BxPC3s/ml. We then calculated the passed through rate for each day of differentiation(figure 3c). Strikingly we found that as the hiPSC-NPCs became further differentiated our removal specificity went away (cells in effluent for day 9 and 12 is similar to control). This suggests the GEDI device captures based on SSEA-5 expression.

To confirm the cells we are catching on the GEDI chip are mostly pluripotent cells with teratoma-forming potential we sent day 12 hiPSC-NPCs and NPCs proliferated for 2 passages (P2 NPCs) as full NPCs through an anti-SSEA-5 GEDI device, respectively. We stained cells caught on the GEDI chip for Oct4, DAPI, and SSEA-3 (a stand in for SSEA-5, due to the inability to use a secondary fluorescent antibody against SSEA-5 on chip (supplementary figure 1a)) (figure 3d). Strikingly, nearly all of the cells caught co-expressed DAPI and SSEA-3 in both the day 12 and P2 NPCs, indicating some level of pluripotency in captured cells. However, in the day 12 sample, a few Oct4+ cells were captured, which were not seen in the P2 sample, indicating further differentiation in the P2 sample, as expected.

1.4 Removal of SSEA-5+ Cells

Having confirmed our device captures cells proportional to SSEA-5 expression, and having confirmed the presence of rare teratoma-forming cells in differentiated populations, we quantified the effectiveness of the GEDI device in removing teratoma-forming cells from a day 9 hiPSC-NPC population by imaging cells in the effluent of anti-SSEA-5 and isotype control functionalized GEDI chips. Strikingly the fraction of cells positive for pluripotency marker SSEA-3 is lower in the SSEA-5 GEDI chip effluent than the control chip effluent for all thresholds (figure 4b), indicating removal of pluripotent cells from the day 9 hiPSC-NPCs. Interestingly the fraction of cells $OCT4^+$ is similar at low to moderate thresholds, then is drastically lower for the SSEA-5 GEDI chip effluent at higher thresholds (figure 4c). Further, the fraction of cells OCT^+ is higher in an absolute sense compared to SSEA-3. An explanation for this may be found in a study of mouse NSCs[35], in which OCT4 expression was found in embryonic day 8.5 (E8.5) whole brain samples, and E9 NSCs. In this study Oct4 was still present at E9, but completely gone by E15.5. However, Oct4 levels in the E9 NSCs was 10^5 fold lower than in mouse ESCs. Therefore an explanation for device performance is that at low thresholds bonafide NPCs (which are similar to NSCs) are counted as $OCT4^+$, but at higher thresholds fewer bonafide NPCs are counted as positive, and thus residual pluripotent cells make up a larger fraction of the $OCT4^+$ cells, of which there are more in the control GEDI chip effluent.

Further, if we aggregate the average fluorescence intensity per nuclei area for the anti-SSEA-5 GEDI chips and isotype control GEDI chips and normalize fluorescence intensity by the respective secondary control we find reduced pluripotency marker expression in the anti-SSEA-5 GEDI chip compared to the isotype control chip (figure 4a). This indicates the anti-SSEA-5 GEDI chip sucessfully removes pluripotency from the day 9 hiPSC-NPC population. Finally, it should be noted that the average intensity per nuclei area in the SSEA-$3_{Anti-SSEA-5groupwas}1.0, suggestingnoexpressionofSSEA-3inthispopulation.$

Discussion

In summary, we have demonstrated that a small residual population of cells expressing pluripotency markers (ie: markers indicative of teratoma-forming potential) exist even after prolonged periods of differentation. To this end we have demonstrated that the GEDI device can successfully reduce this teratoma-forming potential by filtering teratoma-forming cells out of the hiPSC-NPC population.Though future work would require transplanting GEDI-sorted cells into a mouse model, we believe this work represents a promising breakthrough in reducing the teratoma-forming potential of hiPSC-derived therapeutic cells, is generalizable to many hiPSC-dervied cells populations, because pluripotent cells are selected out of the differentiated population in a label free manner, and could be used to increase turn-around time required to derive safe-therapeutic cell

populations. Further we have demonstrated that hiPSCs lose SSEA-5 expression in a more discrete than continuous process, as indicated by drops in fluorescence intensity between day 3 and 6 cells and day 6 and day 9 cells. This suggests there may be optimal time-points at which to filter or sort cells prior to therapeutic transplantation, if one envisions a clinical setting in which therapeutic cells are routinely derived from hiPSCs.

Methods

1.5 Device fabrication and functionalization

Devices were fabricated by A.M. Fitzgerald Associates (Burlingame, CA) according to previously described specifications[32, 36]. The silicon device surfaces were functionalized with a previously described protocol using MPTMS-GMBS-NeutrAvidin-biotin chemistry (Thermo Fisher Scientific, Rockford, IL)[32, 36].The devices were functionalized with primary antibodies via a biotinylation linkage. NeutrAvidin-functionalized devices were incubated with either (1) 2 μg/ml biotinylated mouse anti-human anti-SSEA-5 antibody (Miltenyi Biotec, Bergisch Gladbach, Germany) (2) 10 μg/ml mouse anti-human anti-TRA-1-60 antibody (ThermoFisher Scientific, Waltham, MA), (3) 2 μg/ml of (1) and 10 μg/ml of (2). Control devices were functionalized with biotinylated normal (non-specific) mouse IgG antibodies ((Miltenyi Biotec, Bergisch Gladbach, Germany) at 2 μg/ml. All antibodies were prepared in 2% BSA with 1.3-1.5mM EDTA in PBS. Polydimethysiloxane (PDMS) sheets (5:1 base:curing agent), approximately 3 mm thick, were polymerize for 18 hr at 60and trimmer to form covers for the GEDI device. A PDMS sheet was clamped to the top of the post arrays. Inlet and outlet holes were created with a biopsy punch, and tygon tubing was inserted into the PDMS gasket to connect GEDI chip inlet to a syringe pump and outlet to a microcentrifuge tube for effluent collection. Devices were primed with a 50/50 Ethanol/DI water mixture, and then flushed with DI water water and PBS before experiments.

1.6 Cell Culture

Cell lines[37, 37, 38] were obtained from Tyler Kirby. BxPC3 cells were obtained ATCC (Manassas, VA). All cell lines were cultured in humidified incubators (37 C and 5% CO2) using TeSR-E8 media (StemCell Technologies, Vancouver, Canada) or STEMdiff Neural Induction Medium (StemCell Technologies, Vancouver, Canada) for hiPSCs and hiPSC-NPCs respectively. hiPSC, hiPSC-NPCs, and NPCs were supplemented with 10 μM Y-27632 ROCK Inhibitor for the first day after passaging. DMEM supplemented with 10% FBS and 1% Antibiotic antimycotic for BxPC3s. hiPSCs were harvested after 3–5 days of culture at 60–80% confluency, and differentiating cells were harvested on the stated day.

1.7 Flow cytometry

Cells were trypsinized for 5–7 minutes at 37 °C and then, fixed with 4% v/v paraformaldehyde in PBS for 10-15 minutes. Cells were then permeabilized with 0.1% w/w Saponin in PBS for 5 minutes. Staining was performed with a 1:250 dilution of primary antibody and fluorescently conjugated isotype control antibody in 10% FBS in PBS blocking buffer overnight in the dark at 4°C. Secondary fluorescent antibody was incubated for 1hr at room temperature. For data in which flow cytometry was performed directly after GEDI, cells were stained in primary antibody for 1 hour, then washed. Analysis was performed using a BD Accuri C6 flow cytometer (BD Biosciences, San Jose, CA).

1.8 Capture Experiments

Cells were labeled with 10μM CellTracker Dye, either Green CMFDA or Red CMPTX (Thermo Fisher Scientific, Rockford, IL) for 45 minutes, trypsinized for 5–7 minutes at 37°C and resuspended in carrier solution (2% BSA, 1.3–1.5 mM EDTA in PBS) at approximately 300 cells/ml. Precise counts for each set of experiments were obtained by counting by hand 200ul samples of each cell-suspension-running-buffer mixture. In experiments in which cells were spiked into BxPC3 populations, cultures were trypsinized for 5–7 minutes at 37°C and resuspended in carrier solution at approximately 300,000 cells/ml. Functionalized silicon devices were mounted with Tygon tubing inlets and outlets in a custom PMMA holder. Cell capture was achieved by flowing 0.5 ml of cell suspension through the device at 1 ml/h followed by manual cell enumeration using fluorescence microscopy.

1.9 On-Chip Immunofluorescence

Cells were trypsinized for 5–7 minutes at 37°C and resuspended in carrier solution (2% BSA, 1.3–1.5 mM EDTA in PBS) at approximately 800,000-1,000,000 cells/ml. 0.5 ml of cell suspension was processed through GEDI devices functionalized with anti-SSEA-5 or normal mouse IgG (control) antibodies. Samples were fixed in 2% PFA in 50% PHEM buffer (60 mM PIPES, 25 mM HEPES, 10 mM EGTA and 2 mM MgCl2) for 15 minutes and blocked in 10% FBS in PBS for 1 hour. After staining of surface markers, the samples were permeabilized with 0.1% (w/w) Saponin. The samples were stained with, for Oct4, a primary (Abcam, ab60720,) and an AlexaFluor-488-conjugated secondary antibody (Invitrogen), for SSEA-3, a primary Rat monoclonal to SSEA-3 (Abcam, Ab16286, Lot 1987272) and an AlexaFluor-555-conjugated secondary goat anti-rat antibody

(Abcam, A21434, Lot GR3225471-1) and, for DNA/nuclei, DAPI (Invitrogen). Samples were processed, fixed and stained within 48 h of collection.

1.10 Flow Cytometry Gating

Cells were gated using FlowJo v10 first by identifying cells based on SSC:H vs FSC:H. Single cells were then identified by plotting FSC:A vs FSC:H and gating out cells that did not fit the main linear trend of this plot. 3 biological replicates of undifferentiated hiPSCs were then fit to a normal distribution, and a cutoff threshold for counting cells as SSEA5-$^{+}$ was set at just above the bottom 5% of undifferentiated hiPSCs.

1.11 GEDI Effluent ImmunoFluorescence

3 60mm plates (Corning, CLS430166) of Day 9 hiPSC-NPCs were mixed and pumped through anti-SSEA-5 and isotype control functionalized GEDI chips at 1ml/hr for 30 min. The effluent of each chip (3 of each functionalization) was collected and immeditately fixed for 12 min in 4% w/v PFA. 70% of cells were then stained for Oct4, Nestin, and SSEA-3. 30% of cells received the corresponding secondary fluorescent antibody only. After staining, cells were pipeted and mounted onto glass coverslips coated in alginate hydrogel, to stick the fixed cells to the glass. During mounting, 2 of the secondary control slides (1 SSEA-5 and 1 isotype conrol) were damaged. Cells were then located on slides via the DAPI signal. Each slide was imaged in 3-4 locations on a Zeiss Z710 confocal microscope.

1.11.1 CellProfiler Image Analysis

Quantitative data was obtained by using DAPI signal to locate cells as primary objects in CellProfiler. Secondary objects were then identified using DAPI as seed locations for secondary objects. The total intensity of the secondary object (ie: Oct4 or SSEA-3 intensity) was calculated. Mean Oct4 and SSEA-3 intensity across each of the four conditions (anti-SSEA-5/positive stain, anti-SSEA-5/control stain, isotype control/positive stain, and isotype control/negative stain) for all objects was calculated, and divided by mean DAPI object area for the same condition. Secondary object size was normalized by DAPI area, due to the fact that secondary object area had high variance in the negative stain, due to poorly defined object borders. Mean secondary object positive stain fluorescence intensity normalized by mean secondary object negative stain fluorescence intensity is reported in figure 7. Figure 6 reports the fraction of secondary objects in the positive stain that are a specified fraction brighter than the mean negative stain corresponding secondary object (ie: a threshold of 1.5 means the object is counted as positive if its integrated intensity is at least twice 1.5 times as bright as the average corresponding negative stain object.

References

1. He, Q., Li, J., Bettiol, E. & Jaconi, M. E. Embryonic Stem Cells: New Possible Therapy for Degenerative Diseases That Affect Elderly People. *The Journals Gerontol. Ser. A: Biol. Sci. Med. Sci.* **58**, M279–M287, DOI: 10.1093/gerona/58.3.M279 (2003).

2. Robinton, D. A. & Daley, G. Q. The promise of induced pluripotent stem cells in research and therapy. *Nature* **481**, 295–305, DOI: 10.1038/nature10761 (2012). nature10761.

3. Chhabra, A. Inherent immunogenicity or lack thereof of pluripotent stem cells: implications for cell replacement therapy. *Front. Immunol.* **8**, 1–11, DOI: 10.3389/fimmu.2017.00993 (2017).

4. Serra, M., Brito, C., Correia, C. & Alves, P. M. Process engineering of human pluripotent stem cells for clinical application. *Trends Biotechnol.* **30**, 350–359, DOI: 10.1016/j.tibtech.2012.03.003 (2012).

5. Alzheimer's Association. 2018 Alzheimer's Disease Facts and Figures. *Alzheimers Dement* **14**, 367–429, DOI: 10.1016/j.jalz.2018.02.001 (2018).

6. Kowal, S. L., Dall, T. M., Chakrabarti, R., Storm, M. V. & Jain, A. The current and projected economic burden of Parkinson's disease in the United States. *Mov. Disord.* **28**, 311–318, DOI: 10.1002/mds.25292 (2013).

7. Lunn, S. J., Sakowski, S. a., Hur, J. & Feldman, E. L. Stem Cell Technology for Neurodegenerative Diseases. *NIH Public Access* **70**, 353–361, DOI: 10.1002/ana.22487.Stem (2011).

8. Tuszynski, M. H. *et al.* A phase 1 clinical trial of nerve growth factor gene therapy for Alzheimer disease. *Nat. Medicine* **11**, 551–555, DOI: 10.1038/nm1239 (2005).

9. Herrmann, N., Chau, S. A., Kircanski, I. & Lanctôt, K. L. Current and emerging drug treatment options for alzheimers disease: A systematic review. *Drugs* **71**, 2031–2065, DOI: 10.2165/11595870-000000000-00000 (2011).

10. Schapira, A. H. V. *et al.* Treatment Options in the Modern Management of Parkinson Disease. *Arch. Neurol.* **64**, 1083, DOI: 10.1001/archneur.64.8.1083 (2007).

11. Blurton-jones, M. *et al.* Neural stem cells improve cognition via BDNF in a transgenic model of Alzheimer disease. **106**, 1–6 (2009).

12. Brundin, P., Barker, R. A. & Parmar, M. Neural grafting in Parkinson's disease. Problems and possibilities. *Prog. Brain Res.* **184**, 265–294, DOI: 10.1016/S0079-6123(10)84014-2 (2010).

13. Hargus, G. *et al.* Differentiated Parkinson patient-derived induced pluripotent stem cells grow in the adult rodent brain and reduce motor asymmetry in Parkinsonian rats. *Proc. Natl. Acad. Sci.* **107**, 15921–15926, DOI: 10.1073/pnas.1010209107 (2010). arXiv:1408.1149.

14. Ma, V. Y., Chan, L. & Carruthers, K. J. Incidence, prevalence, costs, and impact on disability of common conditions requiring rehabilitation in the united states: Stroke, spinal cord injury, traumatic brain injury, multiple sclerosis, osteoarthritis, rheumatoid arthritis, limb loss, and back pa. *Arch. Phys. Medicine Rehabil.* **95**, 986–995.e1, DOI: 10.1016/j.apmr.2013.10.032 (2014). NIHMS150003.

15. Thurman, D. J., Alverson, C., Dunn, K. a., Guerrero, J. & Sniezek, J. E. Traumatic brain injury in the United States: A public health perspective. *The J. head trauma rehabilitation* **14**, 602–15, DOI: 10.1097/00001199-199912000-00009 (1999).

16. French, D. D. *et al.* Health Care Costs for Patients With Chronic Spinal Cord Injury in the Veterans Health Administration. *The J. Spinal Cord Medicine* **30**, 477–481, DOI: 10.1080/10790268.2007.11754581 (2007).

17. Blaya, M., Tsoulfas, P., Bramlett, H. & Dietrich, W. Neural progenitor cell transplantation promotes neuroprotection, enhances hippocampal neurogenesis, and improves cognitive outcomes after traumatic brain injury. *Exp. Neurol.* **264**, 67–81, DOI: 10.1016/j.expneurol.2014.11.014 (2015).

18. Lee, H. J. *et al.* Brain transplantation of immortalized human neural stem cells promotes functional recovery in mouse intracerebral hemorrhage stroke model. *Stem cells (Dayton, Ohio)* **25**, 1204–12, DOI: 10.1634/stemcells.2006-0409 (2007).

19. Jeong, S.-W. *et al.* Human Neural Stem Cell Transplantation Promotes Functional Recovery in Rats With Experimental Intracerebral Hemorrhage. *Stroke* **34**, 2258–2263, DOI: 10.1161/01.STR.0000083698.20199.1F (2003).

20. Nagoshi, N. & Okano, H. Applications of induced pluripotent stem cell technologies in spinal cord injury. *J. Neurochem.* **141**, 848–860, DOI: 10.1111/jnc.13986 (2017).

21. Deng, J., Zhang, Y., Xie, Y., Zhang, L. & Tang, P. Cell Transplantation for Spinal Cord Injury: Tumorigenicity of Induced Pluripotent Stem Cell-Derived Neural Stem/Progenitor Cells. *Stem Cells Int.* **2018**, DOI: 10.1155/2018/5653787 (2018).

22. Stevens, K. R. & Murry, C. E. Human Pluripotent Stem Cell-Derived Engineered Tissues: Clinical Considerations. *Cell Stem Cell* **22**, 294–297, DOI: 10.1016/j.stem.2018.01.015 (2018).

23. Press, A. S TEM C ELL T ECHNOLOGY : E PIGENETICS , Whole-Genome DNA Methylation Analyses Revealed Epigenetic Instability in Tumorigenic Human iPS Cell-Derived Neural Stem / Progenitor. 1316–1327 (2017).

24. Barker, R. A., Parmar, M., Studer, L. & Takahashi, J. Human Trials of Stem Cell-Derived Dopamine Neurons for Parkinson's Disease: Dawn of a New Era. *Cell Stem Cell* **21**, 569–573, DOI: 10.1016/j.stem.2017.09.014 (2017).

25. Magown, P., Brownstone, R. M. & Rafuse, V. F. Tumor prevention facilitates delayed transplant of stem cell-derived motoneurons. *Annals Clin. Transl. Neurol.* **3**, 637–649, DOI: 10.1002/acn3.327 (2016).

26. Tang, C. *et al.* An antibody against SSEA-5 glycan on human pluripotent stem cells enables removal of teratoma-forming cells. *Nat. biotechnology* **29**, 829–34, DOI: 10.1038/nbt.1947 (2011). NIHMS150003.

27. Fong, C. Y., Peh, G. S., Gauthaman, K. & Bongso, A. Separation of SSEA-4 and TRA-1-60 labelled undifferentiated human embryonic stem cells from a heterogeneous cell population using magnetic-activated cell sorting (MACS) and fluorescence-activated cell sorting (FACS). *Stem Cell Rev. Reports* **5**, 72–80, DOI: 10.1007/s12015-009-9054-4 (2009).

28. Itakura, G. *et al.* Fail-Safe System against Potential Tumorigenicity after Transplantation of iPSC Derivatives. *Stem Cell Reports* **8**, 673–684, DOI: 10.1016/j.stemcr.2017.02.003 (2017).

29. Doi, D. *et al.* Prolonged maturation culture favors a reduction in the tumorigenicity and the dopaminergic function of human ESC-derived neural cells in a primate model of Parkinson's disease. *Stem Cells* **30**, 935–945, DOI: 10.1002/stem.1060 (2012).

30. Chapman, M. R. *et al.* Sorting single satellite cells from individual myofibers reveals heterogeneity in cell-surface markers and myogenic capacity. *Integr. Biol. (United Kingdom)* **5**, 692–702, DOI: 10.1039/c3ib20290a (2013). 15334406.

31. Menachery, A., Kumawat, N. & Qasaimeh, M. Label-free microfluidic stem cell isolation technologies. *TrAC - Trends Anal. Chem.* **89**, 1–12, DOI: 10.1016/j.trac.2017.01.008 (2017).

32. Kirby, B. J. *et al.* Functional characterization of circulating tumor cells with a prostate-cancer-specific microfluidic device. *PLoS ONE* **7**, 1–10, DOI: 10.1371/journal.pone.0035976 (2012).

33. Zhu, B. *et al.* Microfluidic enrichment of mouse epidermal stem cells and validation of stem cell proliferation in vitro. *Tissue Eng. - Part C: Methods* **19**, 765–773, DOI: 10.1089/ten.TEC.2012.0638 (2013).

34. Boraas, L. C., Guidry, J. B., Pineda, E. T. & Ahsan, T. Cytoskeletal expression and remodeling in pluripotent stem cells. *PLoS ONE* **11**, 1–16, DOI: 10.1371/journal.pone.0145084 (2016).

35. Lee, S. H. *et al.* Dynamic methylation and expression of Oct4 in early neural stem cells. *J. Anat.* **217**, 203–213, DOI: 10.1111/j.1469-7580.2010.01269.x (2010).

36. Gleghorn, J. P. *et al.* Capture of circulating tumor cells from whole blood of prostate cancer patients using geometrically enhanced differential immunocapture (GEDI) and a prostate-specific antibody. *Lab on a Chip* **10**, 27–29, DOI: 10.1039/b917959c (2010).

37. Di Pasquale, E., Song, B. & Condorelli, G. Generation of Human Cardiomyocytes: A Differentiation Protocol from Feeder-free Human Induced Pluripotent Stem Cells. *J. Vis. Exp.* 1–6, DOI: 10.3791/50429 (2013).

38. Di Pasquale, E. *et al.* CaMKII inhibition rectifies arrhythmic phenotype in a patient-specific model of catecholaminergic polymorphic ventricular tachycardia. *Cell Death Dis.* **4**, e843–11, DOI: 10.1038/cddis.2013.369 (2013).

Conflicts of interest

There are no conflicts to declare.

Acknowledgements

The authors would like to acknowledge Tyler Kirby and Jan Lammerding for supplying training in culturing the hiPSC cells.

Author contributions statement

Passed-through experiments in figure 3b were performed by K.W. and C.L. All other experiments were performed by K.W.Data was analyzed by K.W., A.S., and B.K. Experiments were conceived by K.W., A.S., and B.K. K.W. and B.K. wrote the paper.

Additional information

To include, in this order: **Accession codes** (where applicable); **Competing interests** (mandatory statement).

The corresponding author is responsible for submitting a competing interests statement on behalf of all authors of the paper. This statement must be included in the submitted article file.

Figures and tables can be referenced in LaTeX using the ref command, e.g. Figure **??** and Table **??**.

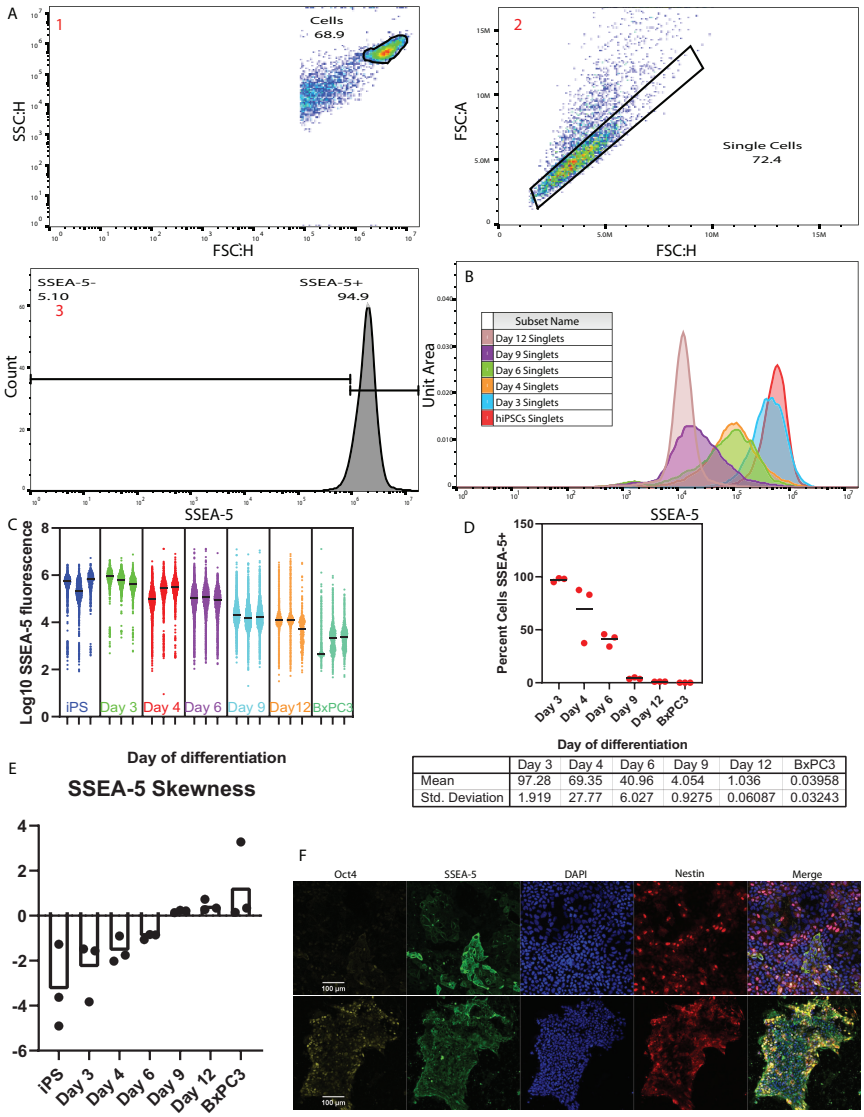

	Day 3	Day 4	Day 6	Day 9	Day 12	BxPC3
Mean	97.28	69.35	40.96	4.054	1.036	0.03958
Std. Deviation	1.919	27.77	6.027	0.9275	0.06087	0.03243

Figure 1. Capture of Rare Teratoma-Forming hiPSCs. (**A**) Gating of single-cells from SSC:H vs. FSC:H to identify cells, FSC:A vs FSC:H to identify single-cells, and thresholding of hiPSCs to identify SSEA-5+ cells (averaged over 3 hiPSCs populations. (**B**) SSEA-5 expression histograms for different time points of differentiation. (**C**) Log10 SSEA-5 Expression for 3 biological replicates at each time point. (**D**) Percent of cells SSEA-5^{+} at each time point. (**E**) Skew of SSEA-5 expression at each time point. (**F**) IF Images of day 9 hiPSC-NPCs (top) and undifferentiated hiPSCs (bottom) (10x).

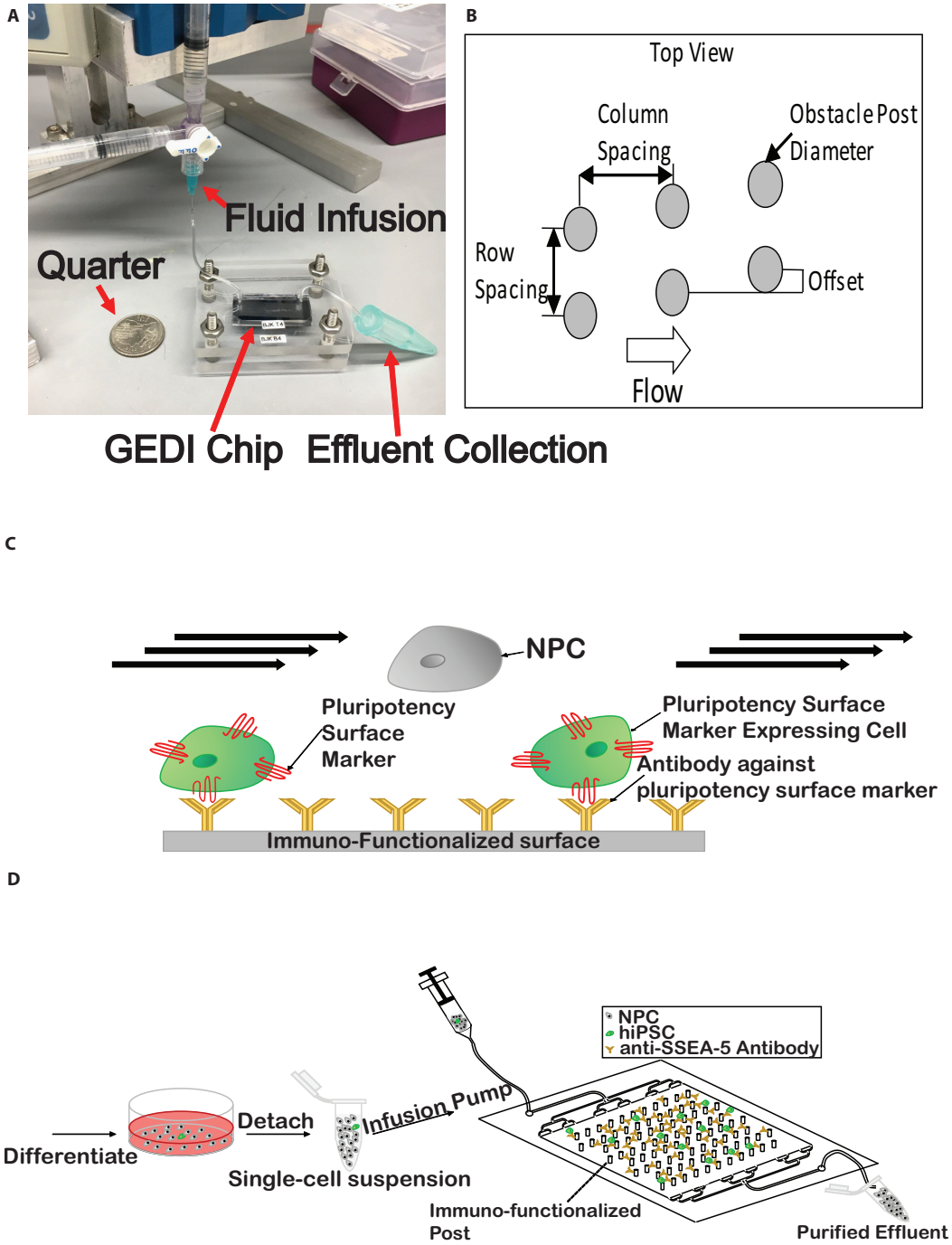

Figure 2. Cartoon Schematic of GEDI device. (**A**) Picture of GEDI chip setup. (**B**) GEDI device schematic (**C**) Cartoon depiction of surface functionalization. (**D**) Overview of GEDI running procedure

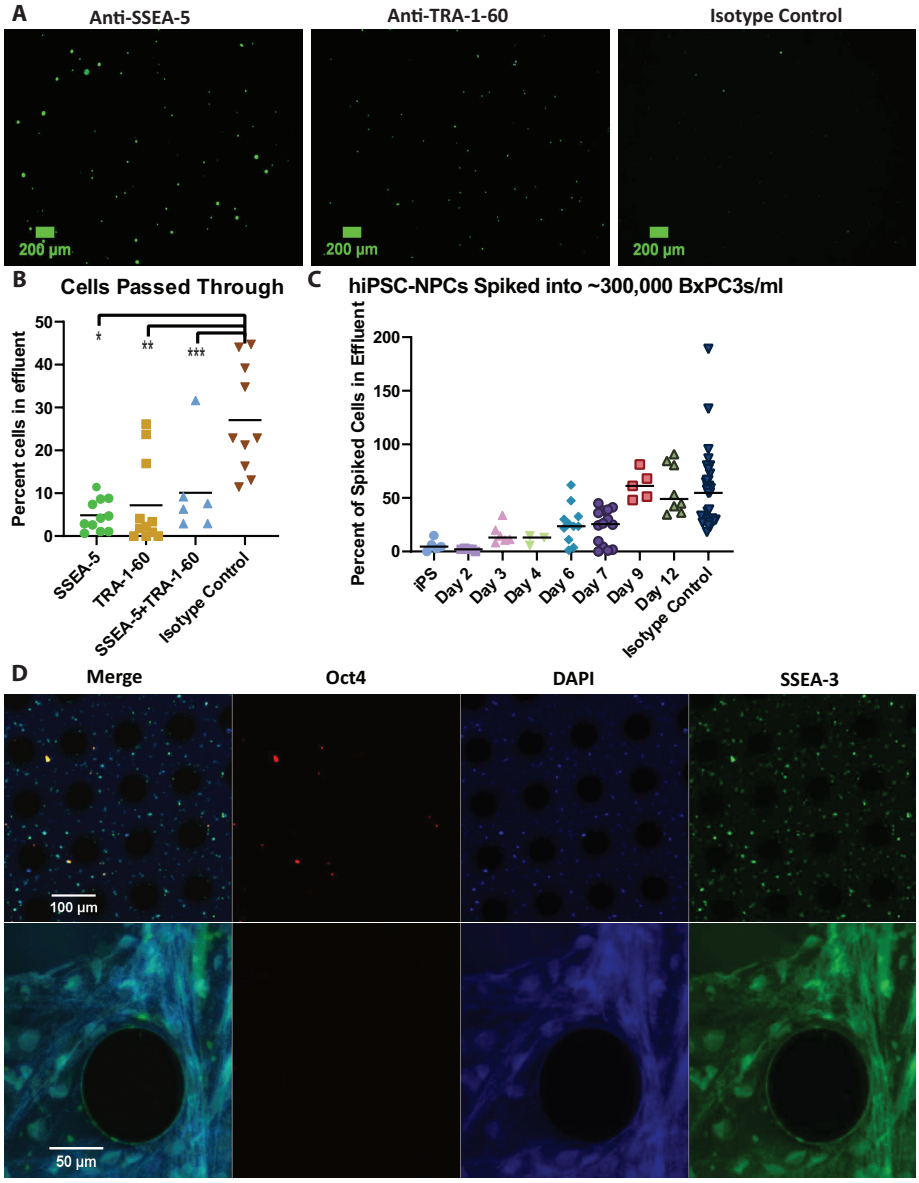

Figure 3. Teratoma-Forming-Cell Capture. (**A**) hiPSCs captured on glass cover-slips with designated antibody surface functionalization. (**B**) Passed through rates for undifferentiated hiPSCs alone in suspension (approx 300 cells/ml sent through) *p<0.0001, **p=0.0002, ***p=0.0088, Tukey's multiple comparison test. (**C**) Passed through rates for hiPSC-NPCs spiked into a larger BxPC3 population at different time points of differentiaiton. (**D**) Immunofluorescence images of cells captured on anti-SSEA-5 GEDI chips. Top: 10x, Day 12 NPCs; Bot: 40x, P2 NPCs (hiPSC differentiated for 5 days, passaged, differentiated for 3 more days, then proliferated through 2 passages in a neural proliferation media.

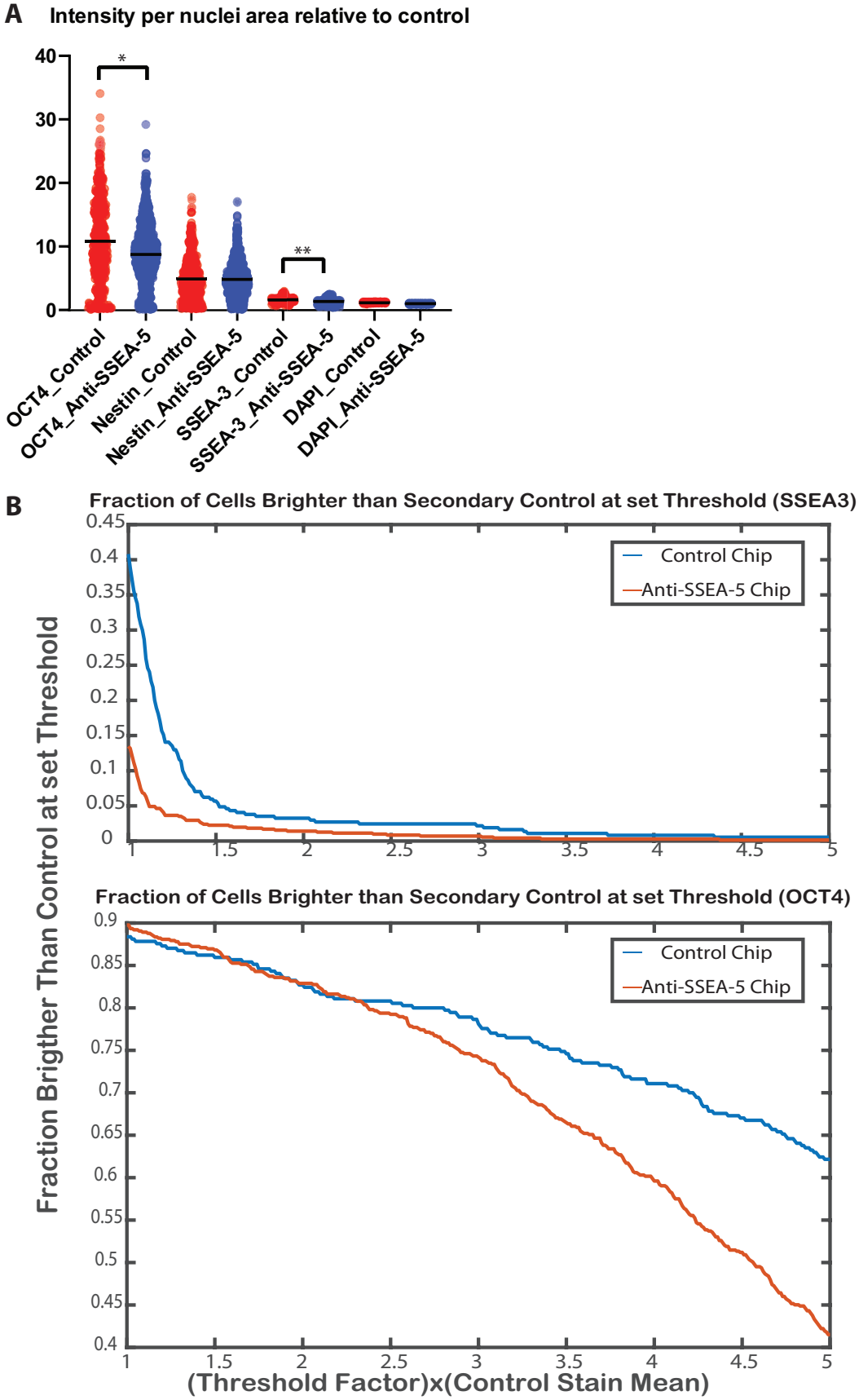

Figure 4. Residual Teratoma-Forming-Cells. (**A**) Expression intensity per nuclei area relative to mean of secondary control for individual cells (117 Outliers removed by ROUT Q=0.1%), *p<0.0001, **p=0.6625, Sidak's multiple comparison test. (**B**) Fraction of day 9 hiPSC-NPCs (a) OCT4^{+} and (b) SSEA-3^{+} in effluent of anti-SSEA-5 and isotype control GEDI chip at varying threshold.

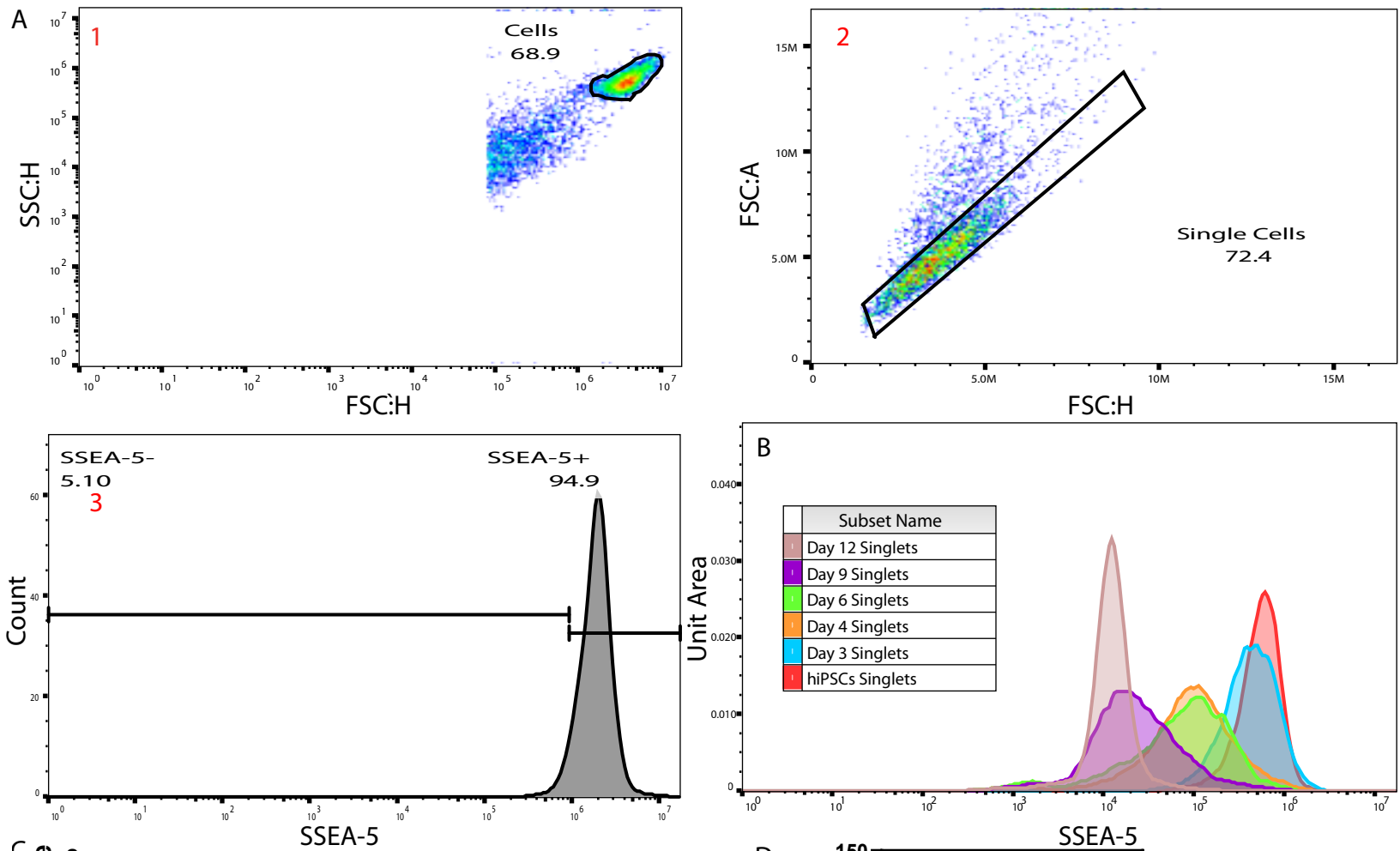

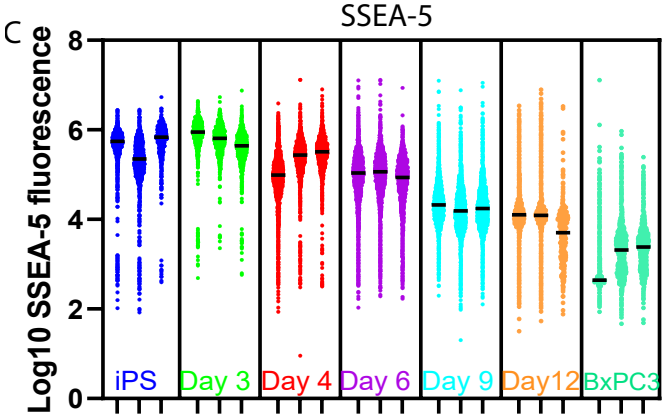

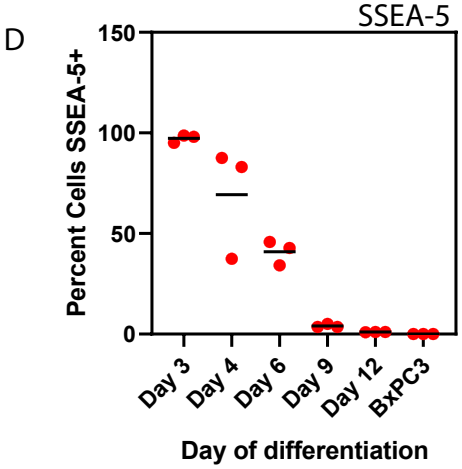

	Day 3	Day 4	Day 6	Day 9	Day 12	BxPC3
Mean	97.28	69.35	40.96	4.054	1.036	0.03958
Std. Deviation	1.919	27.77	6.027	0.9275	0.06087	0.03243

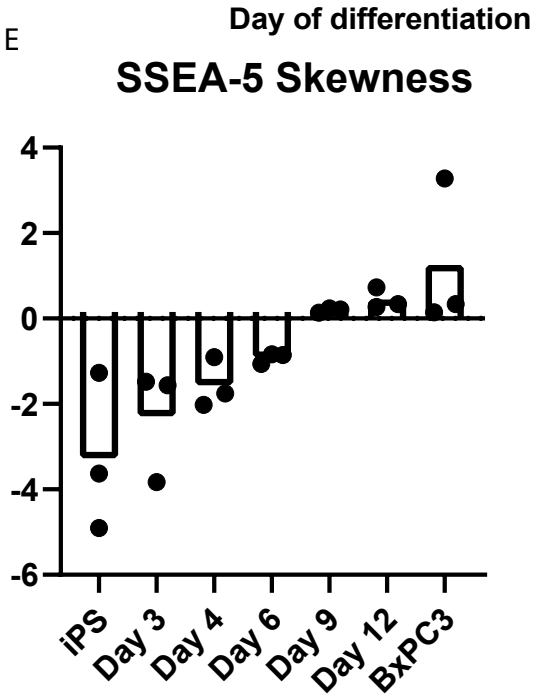

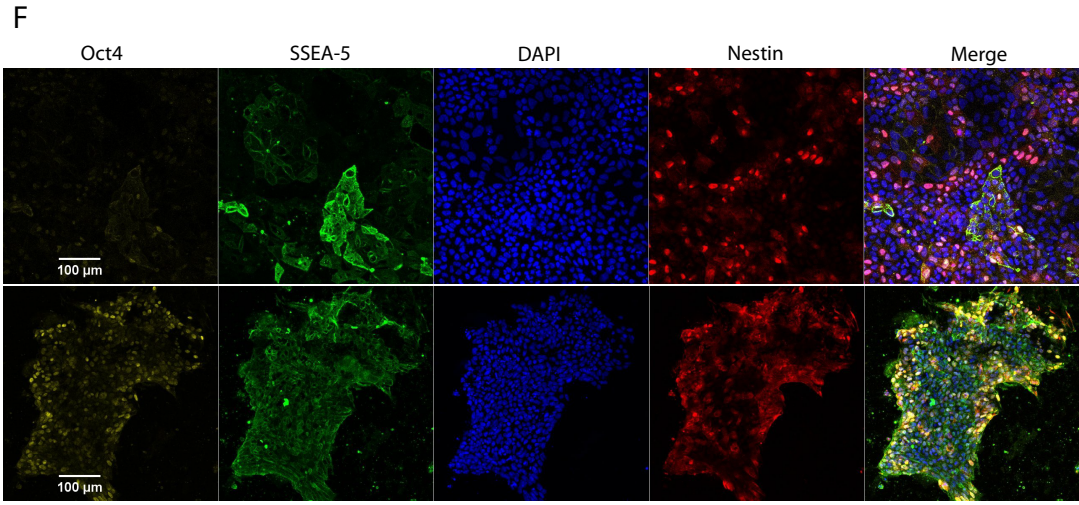

A

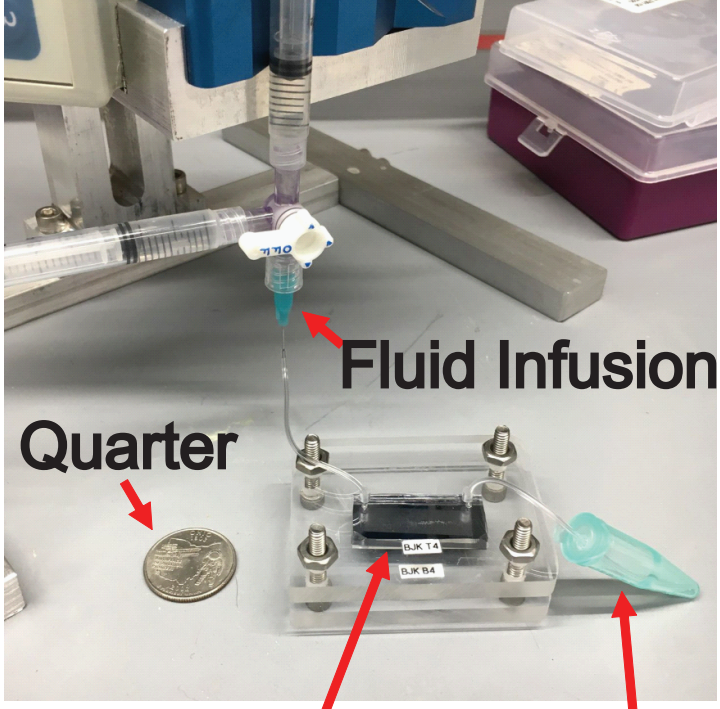
Fluid Infusion
Quarter
GEDI Chip
Effluent Collection

B

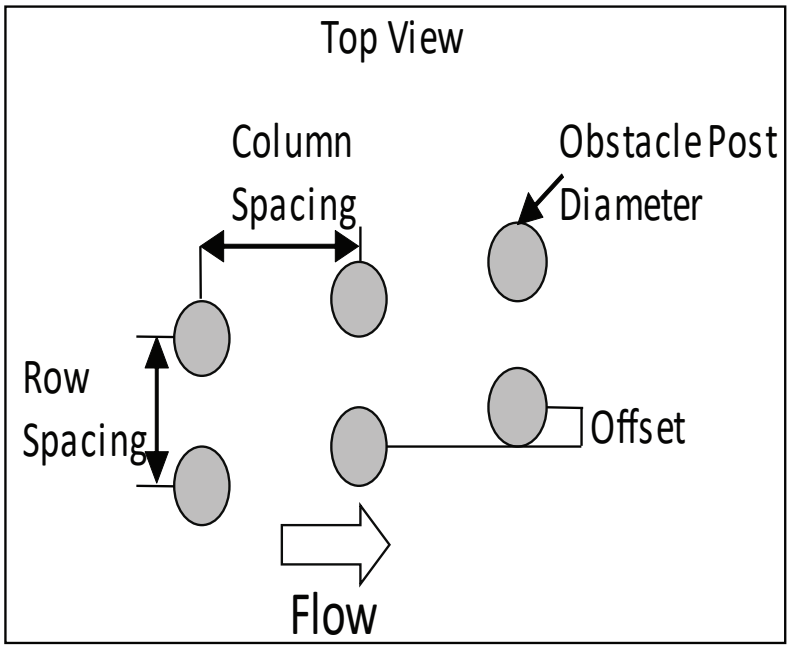
Top View
Column Spacing
Obstacle Post Diameter
Row Spacing
Offset
Flow

C

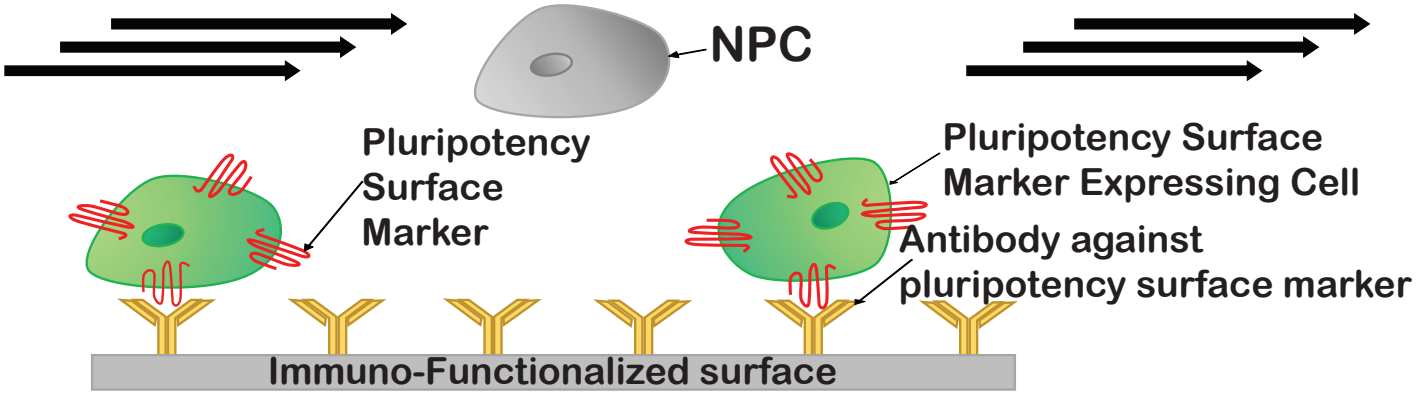
NPC
Pluripotency Surface Marker
Pluripotency Surface Marker Expressing Cell
Antibody against pluripotency surface marker
Immuno-Functionalized surface

D

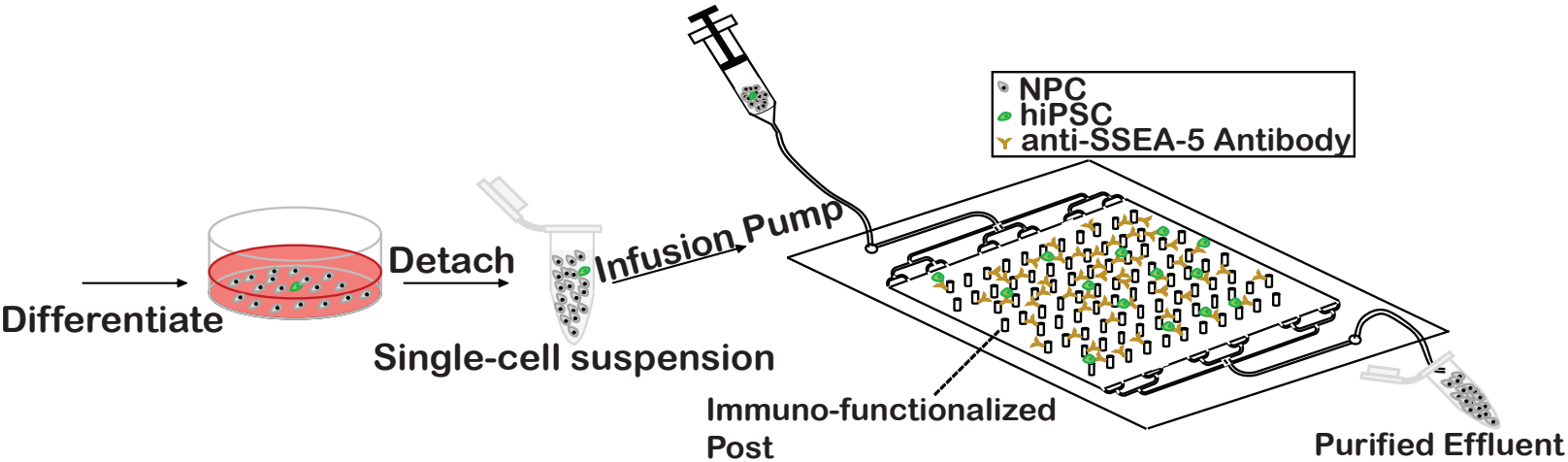
NPC
hiPSC
anti-SSEA-5 Antibody
Differentiate
Detach
Single-cell suspension
Infusion Pump
Immuno-functionalized Post
Purified Effluent

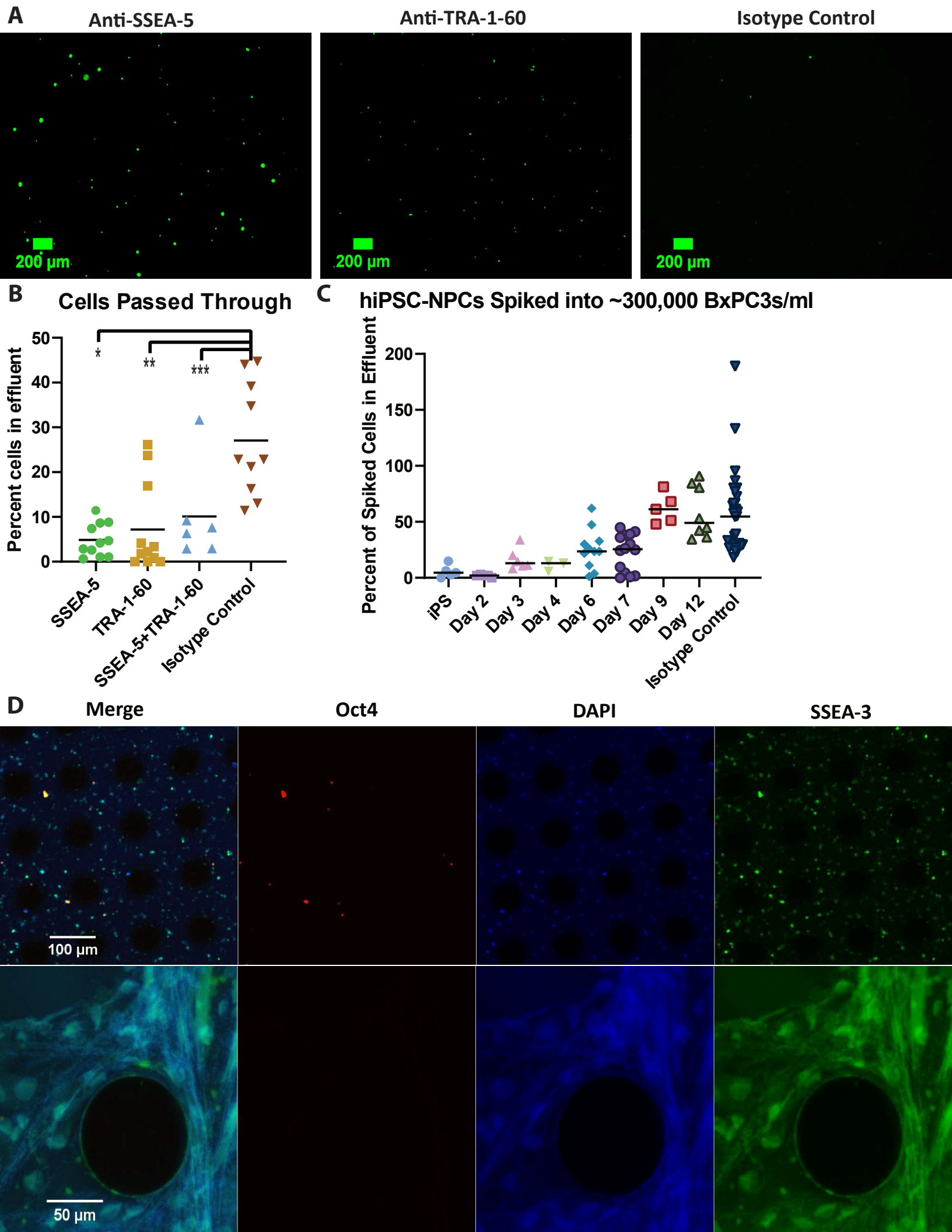
A
Anti-SSEA-5
Anti-TRA-1-60
Isotype Control
200 µm
200 µm
200 µm
B
Cells Passed Through
Percent cells in effluent
50
40
30
20
10
0
*
**
***
SSEA-5
TRA-1-60
SSEA-5+TRA-1-60
Isotype Control
C
hiPSC-NPCs Spiked into ~300,000 BxPC3s/ml
Percent of Spiked Cells in Effluent
200
150
100
50
0
iPS
Day 2
Day 3
Day 4
Day 6
Day 7
Day 9
Day 12
Isotype Control
D
Merge
Oct4
DAPI
SSEA-3
100 µm
50 µm

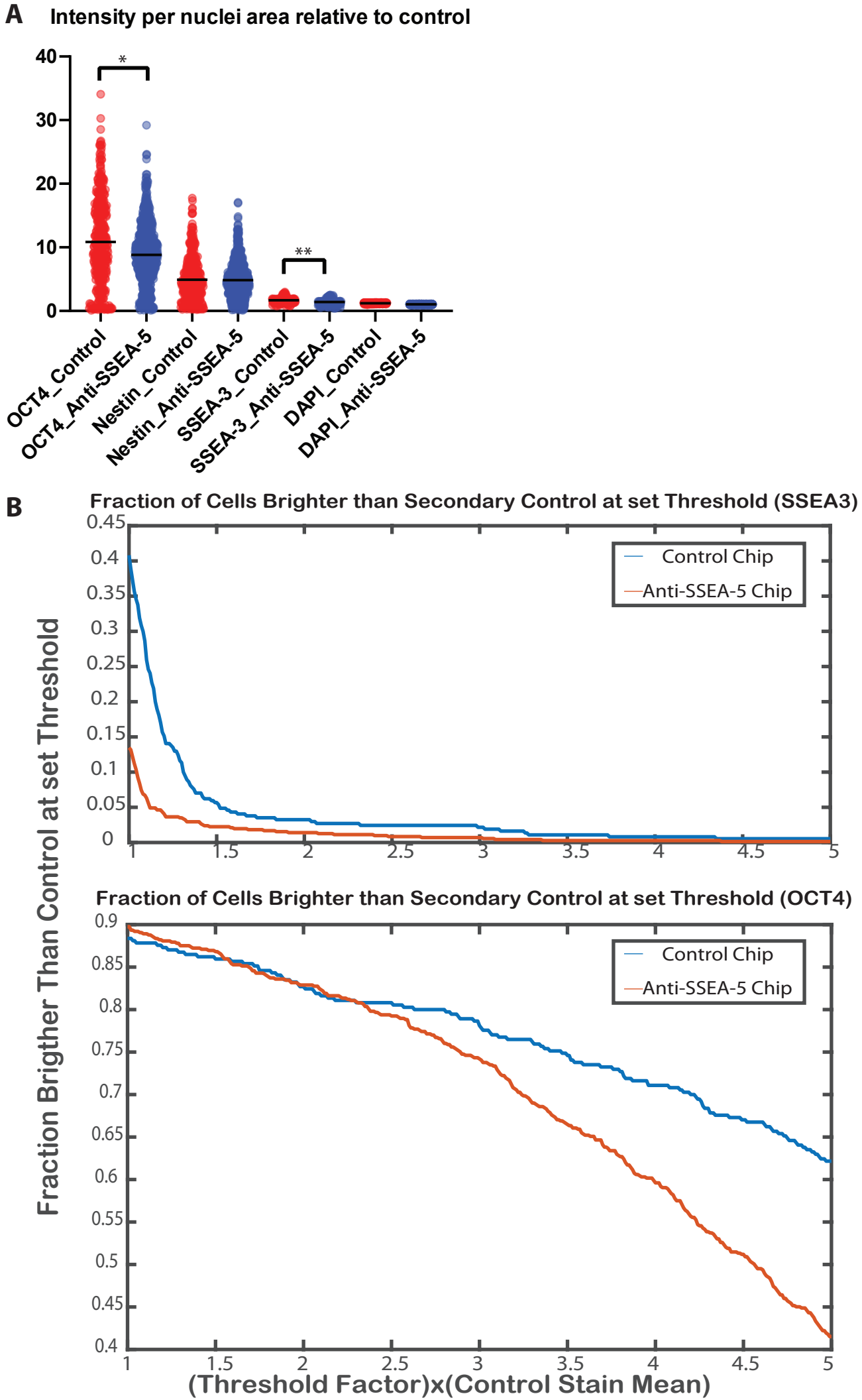
A
Intensity per nuclei area relative to control
40
30
20
10
0
*
**
OCT4_Control
OCT4_Anti-SSEA-5
Nestin_Control
Nestin_Anti-SSEA-5
SSEA-3_Control
SSEA-3_Anti-SSEA-5
DAPI_Control
DAPI_Anti-SSEA-5
B
Fraction of Cells Brighter than Secondary Control at set Threshold (SSEA3)
Control Chip
Anti-SSEA-5 Chip
Fraction Brigther Than Control at set Threshold
Fraction of Cells Brighter than Secondary Control at set Threshold (OCT4)
Control Chip
Anti-SSEA-5 Chip
(Threshold Factor)x(Control Stain Mean)